Switched photonic delay line for phased-array antenna control using externally modulated microwave fiber optic link

Madamopoulos, Nicholas, Riza, Nabeel

Nicholas Madamopoulos, Nabeel A. Riza, "Switched photonic delay line for phased-array antenna control using externally modulated microwave fiber optic link," Proc. SPIE 3160, Optical Technology for Microwave Applications VIII, (23 October 1997); doi: 10.1117/12.283933

SPIE.

Event: Optical Science, Engineering and Instrumentation '97, 1997, San Diego, CA, United States

Switched Photonic Delay Line for Phased Array Antenna Control using Externally Modulated Microwave Fiber-Optic Link

Nicholas Madamopoulos and Nabeel A. Riza

Center for Research and Education in Optics and Lasers * (CREOL)

and the Department of Electrical and Computer Engineering

University of Central Florida

4000 Central Florida Blvd., Orlando, Florida 32816-2700

ABSTRACT

The first demonstration of a 4-bit binary photonic delay line using ferroelectric liquid crystal (FLC) devices and externally modulated S/C band fiber-optic link is presented. A Mach-Zehnder integrated-optic modulator is used to modulate the light. This photonic delay line uses FLC optical on/off devices for optical path switching and active polarization noise filtering. Three dimensional imaging optics and antireflection coated optics are used to minimize photonic delay line insertion losses and interchannel crosstalk. Signal-to-noise ratio measurements as well as interchannel isolation crosstalk analysis is performed.

Keywords: Phased array antennas, photonic beam-forming, photonic delay lines, polarization switching, ferroelectric liquid crystals, external modulation fiber-optic link.

1. INTRODUCTION

Photonic delay lines (PDLs) have become an active area of research. Photonic processing can offer significant advantages such as large instantaneous (several gigahertz) and tunable signal processing bandwidths, along with compact and lightweight processing modules, and protection from electromagnetic interference (EMI) and electromagnetic pulses (EMP). Over the years, several PDL optoelectronic technologies have been proposed for phased array antenna applications [1]. These optoelectronic technologies include bulk optical polarization switched signal control [2,3], wavelength multiplexed time delay systems [4,5], optical gating [6], arrayed optical waveguides [7], and coherent detection methods [8].

Our motivation is to use the mature two-dimensional (2-D) liquid crystal technology for high density polarization switching arrays in conjuction with three-dimensional (3-D) optics to form a multichannel variable PDL for high channel count phased array antennas. We have used both the nematic liquid crystal (NLC) [10,11] and ferroelectric liquid crystal (FLC) [12] technology to form PDLs. Using NLC polarization switching devices we have obtained moderate ly fast switching speeds (1 ms), while maintaining high optical on/off isolation (>35 dB) [10]. Low (<-42 dB) RF interchannel crosstalk has been demonstrated for a single bit 25 channel PDL [13]. The higher switching speed of the FLC devices make FLCs an excellent candidate for advanced phased array antenna applications where higher beam scan rates are required. We have demonstrated fast (35 μs) switching speeds and high optical on/off isolation (>40 dB) for both states of a 1-bit PDL using an active noise filter [12]. Recently we demonstrated a 3-bit FLC based PDL with a directly modulated infrared (1300 nm) semiconductor laser and remote interconnection fiber optics [14]. Antireflection (AR) coated optical components were used to reduce the optical insertion loss to ~1.6 dB per bit. This loss is the attanuatio suffered by the input light to each individual PDL single bit structure. Additional loss occurs from the input and output PDL port coupling optics. Imaging optics were also used to reduce insertion loss due to diffraction as well as minimize interchannel crosstalk.

* N. A. Riza: email: riza@creol.ucf.edu; Tel: (407) 823 6829; Fax: (407) 823 3354

Although direct modulation fiber-optic links are smaller in size and low in cost, they presently have limited dynamic range and frequency response when compered to externaly modulated links. On the other hand, the higher RF gain and lower noise figure of external modukation analog fiber optic links can offer better dynamic range [15]. In this paper we demonstrate for the first time, a 4-bit PDL using FLC devices and an externally modulated fiber-optic link. A Mach-Zehnder integrated-optic modulator is used to modulate the light. Three dimensional imaging optics and antireflection coated optics are used to minimize PDL insertion losses and interchannel crosstalk.

2. THE EXTERNAL MODULATION FIBER-OPTIC LINK FED PHOTONIC DELAY LINE

The experimental set-up of the external modulation fiber-optic link fed PDL is depicted in Fig. 1. A high optical power (250 mW) continuous wave (CW) dioded pumped Nd:YAG laser (λ=1319 nm) is used as the laser source. The laser is connectorized with a polarization maintaining (PM) fiber. A variable optical attenuator is used to contol the optical power of the light before going through the Mach-Zender electro-optic modulator. Then light is launched via a GRIN-lens pigtailed PM fiber into the PDL. All fiber to fiber connections are done using FC/PC connectors. The polarization extinction ratio after the GRIN lens is 30 dB. A high extinction ratio polarizer is used at the input of the PDL. Then the incident light has a polarization extinction ratio of 40 dB. A GRIN-lens pigtail single-mode fiber is used at the output of the PDL to collect and direct the light to the detector.

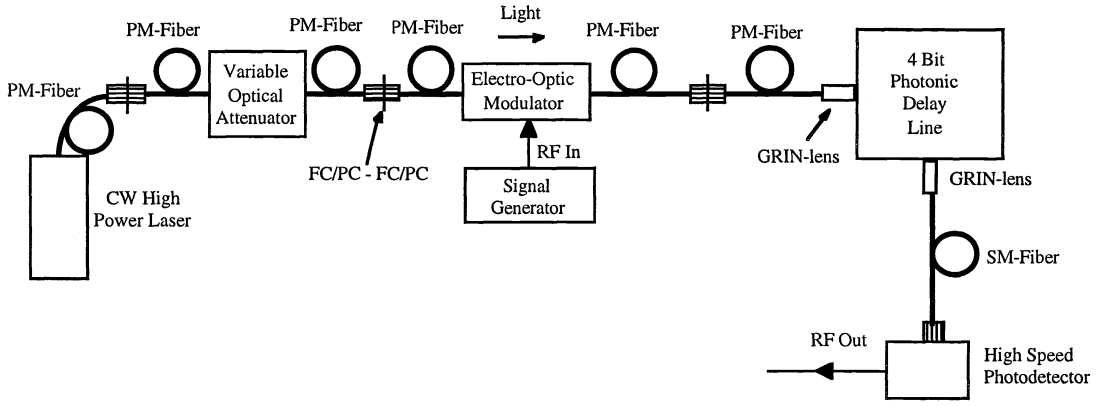

Figure 1: The experimental set-up of the external modulation fiber-optic link fed photonic delay line.

The experimental set-up of the 4-bit PDL line is shown in Fig. 2. The first bit is based on the adaptable PDL design [16]. The delay path consists of a single mode fiber with a Faraday rotator mirror (FR-M) with a total fiber length of 3.15 m. Lenses L1 and L2 are of the same focal lengths. The light travels twice through the fiber and thus gets a relative time delay of 31.5 ns compared with the signal traveling through the other non-fiber path. The second PDL bit is also based on the adaptable PDL architecture. The focal length of lens L3 is 128.032 mm and of lens L4 is 130.8 mm, a 14.95 mm thick glass (OHARA: LAH-58) is used to adjust the delay for the desirable 0.2 ns time delay. The third bit has been designed for a 0.1 ns time delay and is based on the symmetric architecture [17], where the delay and the non-delay paths have the same physical length. Two thick (17.33 mm) glass plates (OHARA: LAH-58) are placed in the delay path to make the optical path longer, and thus obtain the desired time delay. L5 and L6 have focal lengths of 260.040 mm and 256.064 mm respectively. Two half wave plates are placed before the output polarizing beamsplitter cube (PBS) to rotate the polarization of each of the paths by 90°. Hence, each of the two possible signals undergo one reflection and one transmission through the PBSs, thus giving a balanced loss PDL bit performance. The final bit is based on the adaptable PDL architecture and has been designed for 0.4 ns time delay. L7 and L8 have focal lengths of 256.064 mm and 260.04 mm respectively. A glass plate of 39.59 mm thickness is placed in the delay path to create the appropriate optical path length difference between the two paths and give the desired delay of 0.4 ns.

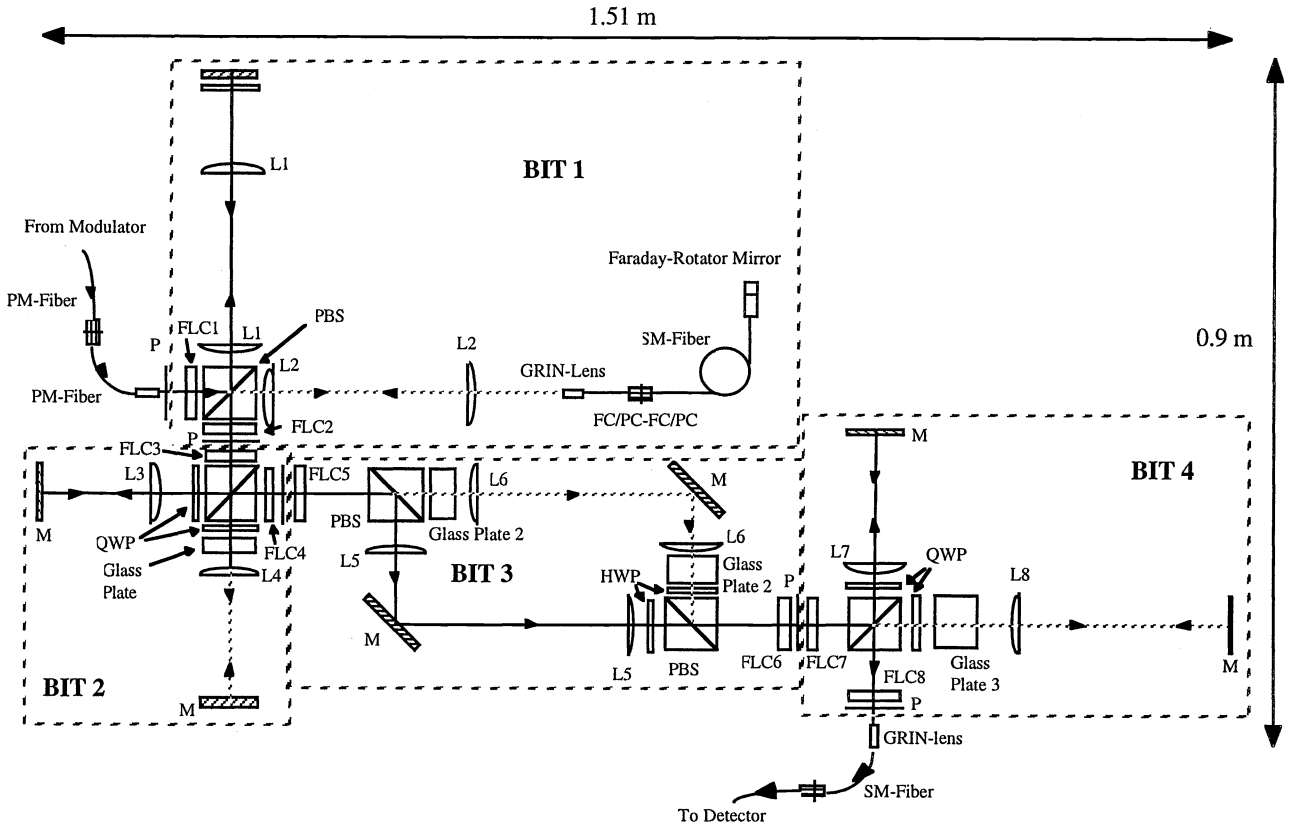

Figure 2: The experimental 4-bit photonic delay line using FLC devices, imaging optics, and fiber-optic remoting. The non-delay paths are represented with solid lines while the delay paths are represented with dashed lines.

Each PDL bit has two FLC polarization switching devices. The first one is used for optical path switching. This FLC acts as a programmable half wave plate that either rotates the incident polarization by 90° or leaves the polarization unaffected. Depending on the SOP of the light, the switched optical beam can follow either the delay or non-delay path. The second FLC device along with a high extinction ratio polarizer form the active noise filter that supresses any noise leakage from the first FLC device and the PBS. The two FLC devices are chosen to operate out of phase. That means that whenever one is set "on" and thus rotates the incident polarization the other one is set "off" and leaves the polarization unaffected [12]. This out of phase operation has been found to give lower leakage noise levels for our PDL modules [12].

3. PHOTONIC DELAY LINE OPTICAL LOSS BUDGET

One of the main issues of any PDL is optical insertion loss. We propose the use of AR coated optical components to reduce the optical insertion loss of our PDL. Table 1 shows the expected and measured optical loss for both settings of each of the PDL bits. The expected optical insertion loss was calculated based on the optical component loss values given by the manufacturers, and the measured optical losses for the FLC devices.

From Table 1 we can see that the losses are at the expected levels. Overall, our optical insertion loss numbers are limited from the rather high loss of the FLC devices. The measured typical optical loss for our FLC devices is 0.7 dB. Considering that each PDL bit has two FLC devices, a 1.4 dB loss is due to the FLC devices. This high loss is due to the fact that the FLC devices consist of a cascade of three FLC cells, each sandwitched between two glass plates. Triple cells are used because of the current limitation of the manufacturer to provide thick enough single cell FLC devices that can rotate the polarization by 90° at the required 1319 nm wavelength. It is anticipated that as technology develops and new FLC materials are synthesized, double cell or single cell FLC devices

with lower insertion losses (~ 0.3 dB) will become available. This will further reduce the optical insertion loss of our PDL by ~ 0.8 dB per bit, implying a typical 1 dB optical insertion loss per bit. The measured optical loss for the 16 settings of our 4-bit PDL are shown in table 2. These measurements were obtained using an optical power meter at the output of the PDL.

Table 1: Expected and measured optical insertion loss for the binary settings of each of the four PDL bits.

	Non-Delay		Delay	
# Bit	Expected Optical Loss (dB)	Measured Optical Loss (dB)	Expected Optical Loss (dB)	Measured Optical Loss (dB)
1	1.72	1.66	4.28	4.50
2	2.02	1.90	2.04	1.98
3	1.99	1.91	2.01	1.94
4	1.81	1.90	1.96	2.00

Table 2: Average PDL opical loss

PDL Setting				Measured Optical Loss (dB)	PDL Setting				Measured Optical Loss (dB)
Bit 1	Bit 2	Bit 3	Bit 4		Bit 1	Bit 2	Bit 3	Bit 4	
N	N	N	N	7.35	D	N	N	N	10.71
N	N	N	D	7.46	D	N	N	D	10.77
N	N	D	N	7.38	D	N	D	N	10.79
N	N	D	D	7.15	D	N	D	D	10.86
N	D	N	N	7.29	D	D	N	N	10.62
N	D	N	D	7.41	D	D	N	D	10.73
N	D	D	N	7.35	D	D	D	N	10.64
N	D	D	D	7.49	D	D	D	D	10.77

4. THE FIBER INTERCONNECTION ISSUE

Another important issue in our PDL is the output optical coupling system. The PDL consists of 4 bits, and thus has sixteen different settings. The signals of those settings travel through sixteen different path combinations. All these different signals have to be effectively collected and detected. Since fiber remoting is proposed to distribute the processed optical signals to the photodetectors, a large area (1.8 mm in diameter) GRIN-lens pigtailed fiber can be used to maximize the optical coupling efficiency. We have previously proposed the use of a GRIN-lens pigtailed single-mode fiber as the collecting element [18]. The coupling losses associated with the GRIN-lens pigtailed single-mode fiber make this approach rather intensive since all sixteen settings have to be collinear at the output of the PDL. Another approach is to use a GRIN-lens pigtailed multi-mode fiber. The larger fiber size (core diameter 50 μm) of the multi-mode fiber can give greater collecting power and can thus make the system less sensitive to small optical misalignments.

Two sets of measurements were performed, one using a GRIN-lens pigtailed single-mode fiber (9 μm core diameter) and another using a GRIN-lens pigtailed multimode fiber (50 μm core diameter). The measurements were performed using an optical power meter to detect the light at the output end of the fiber that would eventually connect to a photodetector. The average coupling loss for the 16 settings of the PDL when the single-mode fiber was used was 2.0 dB. When the multi-mode fiber was used, the coupling loss reduced to 0.5 dB. This 1.5 dB optical coupling efficiency improvement will eventually give a 3.0 dB RF gain to the signal when a multi-mode fiber is used. Experiments were also performed using a 200 μm core diameter multi-mode fiber. No improvement was observed in the optical coupling efficiency of the output port fiber coupling system compared with the 50 μm fiber.

5. THE LEAKAGE NOISE ISSUE

Another system issue of the PDL is the within channel leakage noise, or the signal-to-noise ratio (SNR) issue. Electrical SNR is defined as 20log(signal power/noise power). As signal, we define the optical power in the optical beam that travels through the desired PDL path setting; all other optical power measured at the output is regarded as noise optical power. Table 3 shows the RF SNR values for the 16 settings of the PDL. Both a single-mode (9 μm core diameter) and a multi-mode (50 μm core diameter) fiber were used at the PDL output port to obtain the measurements. From Table 3 it can be seen that the PDL electrical leakage noise is less than -70 dB for all 16 time delay settings, using either of the output port coupling systems. The use of the multi-mode fiber does not degrade the SNR

performance of the PDL. Thus, in conjunction with the higher optical coupling efficiency that provided by the multi-mode output fiber, it is the preferred coupling output fiber.

Table 3: Electrical SNR values of the PDL using (a) GRIN lens pigtailed single-mode fiber and (b) GRIN lens pigtailed multi-mode fiber coupling system.

PDL Setting				Electrical Leakage Noise-based SNR (dB)	
BIT1	BIT 2	BIT 3	BIT 4	Single-mode Fiber Coupling System	Multi-mode Fiber Coupling System
N	N	N	N	79.18	78.80
N	N	N	D	79.03	78.67
N	N	D	N	90.68	88.09
N	N	D	D	89.82	86.00
N	D	N	N	74.15	73.78
N	D	N	D	73.98	74.08
N	D	D	N	79.46	78.70
N	D	D	D	79.68	80.11
D	N	N	N	75.41	76.18
D	N	N	D	75.51	77.67
D	N	D	N	74.02	76.90
D	N	D	D	73.94	77.95
D	D	N	N	71.48	70.29
D	D	N	D	71.95	70.46
D	D	D	N	73.82	74.08
D	D	D	D	74.15	73.64

6. RF POWER MEASUREMENTS AND DYNAMIC RANGE LOSS COMPENSATION METHODS

The electro-optic modulator (UTP, APE MZM-1.3-8-T) was fed by a 6 GHz, 11.98 dBm RF power level signal from our HP 83752A signal generator. The carrier to noise ratio (C/N) of this input RF signal measured at 100 KHz offset was 107.0 dB/Hz (Fig. 3).

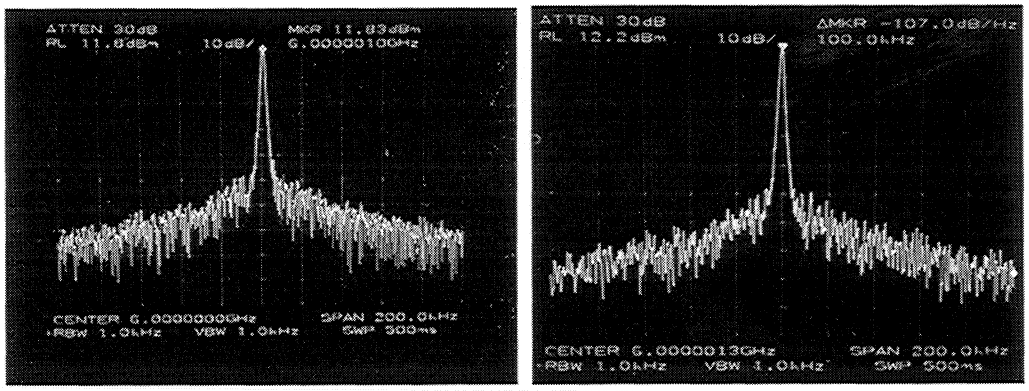

(a) (b)

Figure 3: RF spectrum analyzer traces at 6 GHz showing (a) the 11.98 dBm RF signal fed to the electo-optic modulator; (b) its 107 dB/Hz C/N measured at 100KHz offset.

First the performance of the externally modulated fiber-optic link without the PDL was tested. The optical attenuator in the fiber optic link was adjusted so that a 3 mW optical power level is incident on the photodetector. The RF gain of the externally modulated fiber-optic link is shown in Fig. 4. The fiber-optic link exibits a -42 dB RF gain (or a 42 dB RF loss). The dynamic range remains near the same level, i.e., at 104.2 dB/Hz (Fig. 4 (b)).

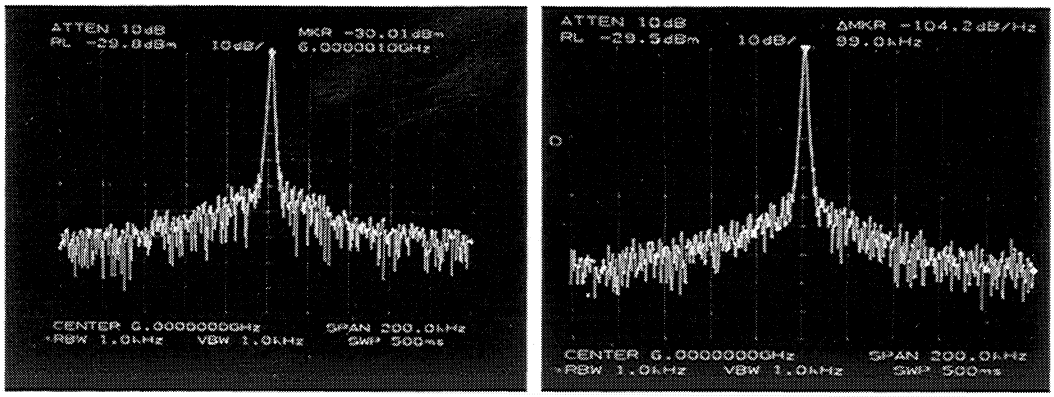

(a) (b)

Figure 4: RF spectrum analyzer traces showing the 42 dB RF loss of the externally modulated 6 GHz fiber-optic link. (a) RF power drops at -30.01 dB, (b) a 140.2 dB C/N is measured at 100KHz offset .

When the PDL is inserted into the externally modulated link path via the use of fiber-to-free space coupling optics an extra RF loss is expected. A single-mode fiber was used at the output of the PDL because a single mode connectorized photodetector was available. Fig. 5 shows an additional RF loss of 19.16 dB of the externally modulated fiber-optic link due to the PDL (PDL setting: zero delay). Note that this RF loss also causes the dynamic range to drop by ~ 19 dB.

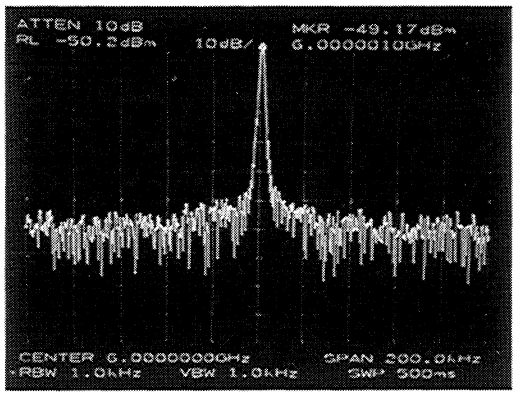

Note Drop in Dynamic Range by ~19 dB

PDL Setting Optical Loss: 7.35 dB (measured)
Input Optical Fiber and Input Polarizer Optical Loss: 0.1 dB (measured)
Output SM-Fiber Coupling Loss: 1.8 dB (measured)
One additional FC/PC Connector: 0.25 dB (typical)

} Expected RF Loss 19.00 dB

Figure 5: Spectrum analyzer trace showing a 19.16 dB RF loss of the 6 GHz fiber-optic link with the PDL set for zero delay. This 19.60 dB RF loss is consistent with the expected RF loss based on the optical losses due to the PDL setting, the input polarizer, output single-mode fiber and the additional FC/PC connector.

The dynamic range of the signal should be kept at the same level after propagation of the signal through the PDL. This is particularly important in the receive mode of the photonic beamformer as signals coming from the antenna elements are lower in power. In the following section, we describe and test a method for dynamic range loss compensation.

The dynamic range loss compensation method is based on an electrically controlled optical attenuator before the electro-optic modulator. This attenuator is set such that the incident optical power after propagation and attenuation through the PDL is at levels

required from the detector for maximum photodetected dynamic range. Fig. 6 shows such a configuration where the optical attenuator is computer controlled depending on the levels of detected RF power. For PDL calibration purposes on a day-to-day basis, the RF power splitter sends a small portion of the RF power to the power meter and with the help of a computer and a data base, the appropriate feedback signal is sent to the attenuator for fine control. Because the PDL loss for each bit setting is known, the attenuator settings are also known a priori.

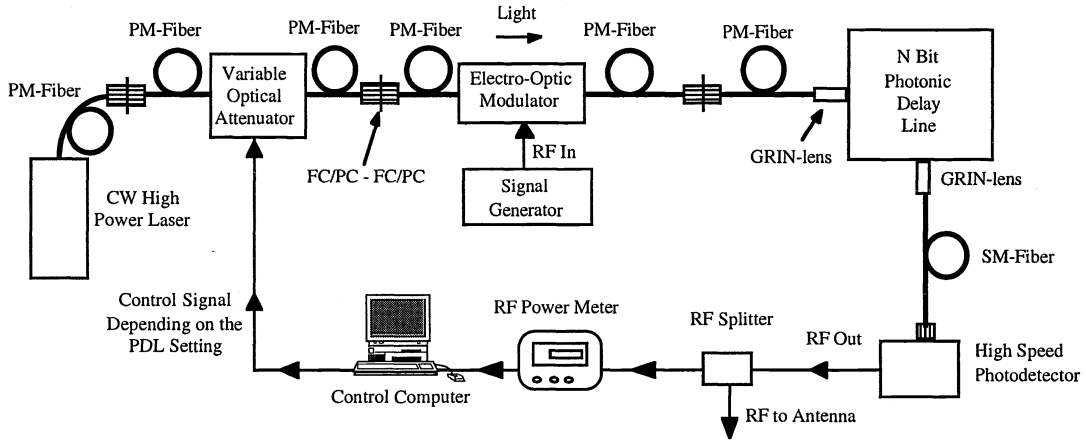

Figure 6: Dynamic range loss compensation method based on apriori controlled optical attenuation.

In our experiment, the optical attenuation of the laser light was reduced by 9.5 dB using the variable attenuator. The RF power detected reached the initial value of -30.00 dBm and the dynamic range also got higher and approached its original value at 104.00 dB, as shown in Fig. 7.

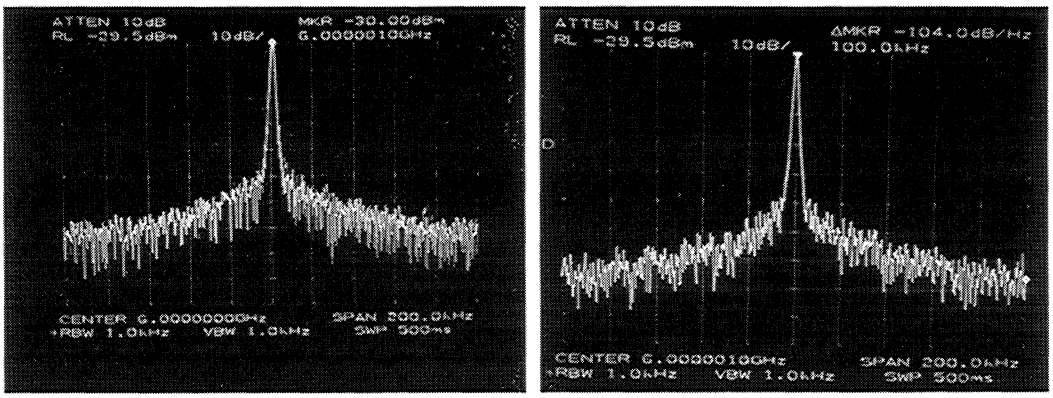

(a) (b)

Figure 7: RF spectrum analyzer traces showing the dynamic range loss compensated 6 GHz (a) RF power at -30.00, and the (b) 104.0 dB C/N measured at 100 KHz offset.

Note that the PDL does not degrade the C/N of the signal. As C/N degradation we define the difference between the C/N when the PDL is not included in the link path and when the link is included in the link path. Overall the C/N degradation for our PDL over the 16 time delay settings is 2 dB.

The dynamic range loss compensation method can be combined with post-amplification of the photodetected signal so that the RF power level can reach higher values such as those required for phased array antenna applications. Again the optical attenuation of the laser light was reduced by 9.5 dB. A 22 dB RF amplifier (Mini Circuit: Z-RON8) is used to amplify the photodetected signal. This time, the RF signal reaches -8.33 dBm (Fig. 8(a)), and the dynamic range rises close to its original value at 103.8 dB/Hz (Fig. 8 (b)).

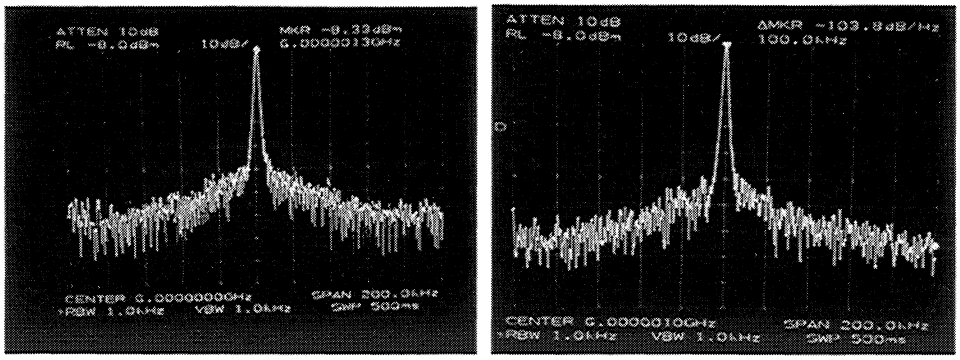

(a) (b)

Figure 8: RF spectrum analyzer traces 6 GHz showing (a) the RF power at -8.33 dBm, and (b) the 103.8 dB/Hz C/N measured at 100 KHz offset.

7. S-BAND OPERATION OF THE EXTERNALLY MODULATED PDL

One of the advantages of photonic beamforming is the ability to change RF frequency of operation over wide bandwidths without essentially changing any of the hardware. All previous experimental demonstration was rerformed at 6 GHz. Fig. 9 shows operation at 3 GHz. Fig 9 shows a 12.17 dBm, 108 dB/Hz C/N signal that is fed into the electro-optic modulator. Fig 10 shows the post amplified photodetected signal. The PDL was set for zero time delay and the optical attenuator was set a 9.5 dB gain higher optical power compared to the link without the PDL.

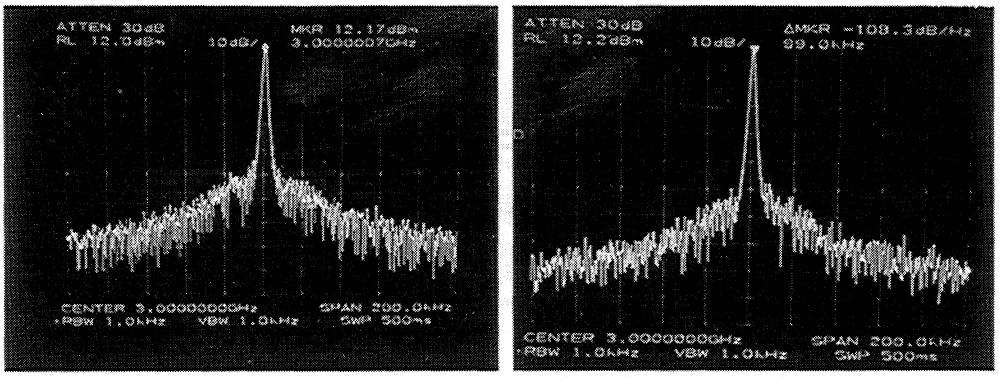

(a) (b)

Figure 9: RF spectrum analyzer traces of the 3 GHz signal fed into the electro-optic modulator (a) RF power: 12.17 dBm, and (b) C/N: 108.3 dB/Hz measured at 100 KHz offset.

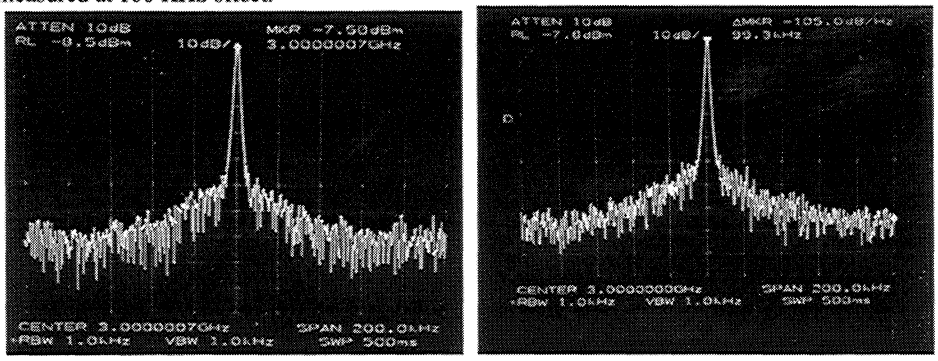

(a) (b)

Figure 10: RF spectrum analyzer traces of the 3 GHz photodetected signal after post amplification (a) RF power: -7.50 dBm, and (b) C/N: 105.0 dB/Hz measured at 100 KHz offset.

8. TIME DELAY MEASUREMENTS

Time delay measurements were also obtained for the 4-Bit PDL. As mentioned earlier the second, third and fourth bits in the PDL have been designed for a 0.2 ns, 0.1 ns, and 0.4 ns time delay, respectively. Fig. 11 shows, the measured time delays obtained from the second, third and fourth bits respectively. The top traces show the non-delayed 6 GHz signal and the bottom traces show the 6 GHz delayed signals. The measured values are shown in Fig. 11; (a) 0.270 ns, (b) 0.105, and (c) 0.425 ns. This difference from the designed time delays is due to tolerances due to the lens and glass fabrication process as well as due to small displacement errors of the optical components in the delay or non-delay paths. The laser source used in the experiment has a longitudinal mode spacing of 4.5 GHz. This causes the 6 GHz signal on the oscilloscope to have some ripples.

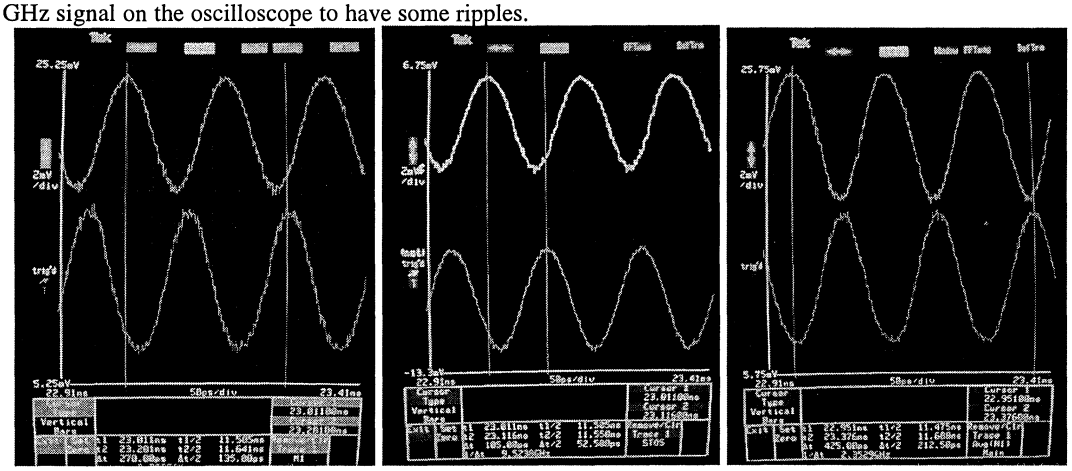

(a) (b) (c)

Figure 11: Oscilloscope traces at 6 GHz showing a (a) 0.270 ns, (b) 0.105 ns, and (c) 0.425 ns time delay for the second, third and fourth PDL bits. Top traces: the non-delayed signal, bottom traces: the delayed signal.

9. INTERCHANNEL CROSSTALK

Interchannel crosstalk measurements were also obtained for our PDL. As interchannel crosstalk, we define the optical power leaking from one channel to the adjacent ones. Since the signal of interest is the time delayed or non-delayed signal, leakage from one channel to the adjacent ones that do not carry the same delay "information" will be translated to noise, and this will deteriorate the system performance. In the experimentally demonstrated PDL, there is only one active channel. Thus, in order to take the interchannel crosstalk measurements, the output GRIN lens of the multi-mode fiber coupling system was translated in the two orthogonal directions of the output plane (-x and -y) in steps of 1.8 mm, which is the typical diameter of the GRIN lens. The total translation in each direction was 7.2 mm which corresponds to five GRIN-lens positions. One position is at the center, and the others are at 1.8 mm and 3.6 mm from each side of the center GRIN-lens. This 7.2 mm span was used because in our system we used 10 mm active area polarizers. Fig. 12 shows typical interchannel crosstalk values. Note that a worst case leakage noise of -42 dB was measured in the adjacent channel, which leads to an RF interchannel crosstalk of - 84 dB.

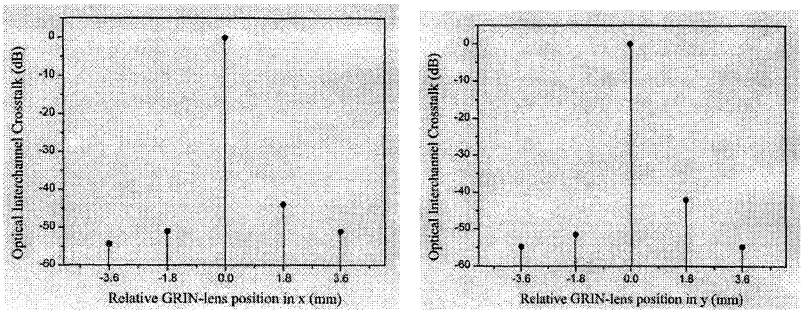

(a) (b)

Figure 12: Optical interchannel crosstalk relative to the center active channel when the PDL is for maximum delay setting, with measurements taken along the (a) x and (b) y directions at the PDL output plane. A maximum optical interchannel crosstalk of -42.1 dB (or -84.2 dB RF) is measured at the nearest to center channel in the y-direction.

10. CONCLUSION

We have demonstrated for the first time, a 4-bit PDL using ferroelectric liquid crystal devices and externally modulated S/C band fiber-optic link for fiber remoting. An average low PDL RF leakage noise (<-77 dB) over the 16 time delay settings was demonstrated. Low 1.9 dB/bit average optical loss was measured, which can be further reduced to ~1 dB using lower loss (0.3 dB) FLC devices. We have also demonstrated an RF gain of 3 dB with a multimode fiber output port versus a single-mode fiber output port. A ~105 dB/Hz dynamic range was also maintained by our PDL system, which is consistent with the generator signal quality driving the integrated-optic modulator. The C/N degradation due to the PDL in the externally modulated fiber-optic link path was estimated at 2 dB. Low interchannel RF crosstalk (averaged <-84 dB) was measured relative to the center active channel of the PDL.

ACKNOWLEDGMENTS

This work is supported by grant #N000149510988 from the Office of Naval Research, Program Monitor, Dr. Miceli.

REFERENCES

1. N. A. Riza, Editor, *Selected Papers on Photonic Control of Phased Array Antennas*, *SPIE Milestone Series*, Vol. MS 136, June, 1997
2. N. A. Riza, "Transmit/receive time-delay beam-forming optical architecture for phased array antennas," *Applied Optics*, Vol. 30, No. 32, pp. 4594-4595, November 1991.
3. D. Dolfi, P. Joffre, J. Antoine, J.-P. Huignard, D. Philipet, and P. Granger, "Experimental demonstration of a phased array antenna optically controlled with phase and time delays," *Applied Optics*, Vol. 35, No. 26, pp. 5293-5300, September 10, 1996.
4. A. P. Goutzoulis and D. K. Davies, "Hardware-compressive 2-D fiber optic delay line architecture for time steering of phased array antennas," *Applied Optics*, Vol. 29, No. 36,pp. 5353-5359, December 20, 1990.
5. N. A. Riza and N. Madamopoulos, "Phased-array antenna, maximum-compression, reversible photonic beam former with ternary designs and multiple wavelengths," *Applied Optics*, Vol. 36, No. 5, pp. 983-996, February 10, 1997.
6. Cohen, Y. Chang, A. F. J. Levi, H. R. Fetterman, and Irwin L. Newberg, "Optically controlled serially fed phased array sensor," *IEEE Photonics Technology Letters*, Vol. 8, No. 12, pp. 1683-1685, December 1996.
7. Yegnanarayanan, P. D. Trinh, and B. Jalali, "Recirculating photonic filter: a wavelength-selective time delay for phased-array antennas and wavelength code-division multile access," *Optics Letters*, Vol. 21, No. 10, pp. 740-742, May 15, 1996.
8. P. M. Freitag and S. R. Forrest, "A coherent optically controlled phased array antenna system," *IEEE Microwave and Guided Wave Letters*, Vol. 3, No. 9, pp. 293-295, September 1993.
9. N. A. Riza, and N. Madamopoulos, "Phased array antenna maximum compression reversible photonic beamformer using ternary designs and multiple wavelengths," *Applied Optics*, Vol. 36, No. 5, pp. 983-996, 10 February, 1997.
10. N. A. Riza, "High-optical-isolation low-loss moderate-switching-speed nematic liquid-crystal optical switch," *Optic Letters*, Vol. 19, No. 21, pp. 1780-1782, Nov. 1, 1994.
11. N. A. Riza, and N. Madamopoulos, "Microwave band demonstration of a reflective geometry fiber and free-space binary photonic delay line," *Microwave Guided Letters*, Vol. 7, No. 4, pp. 103-105, April, 1997.
12. N. A. Riza, N. Madamopoulos, "Characterization of a ferroelectric liquid crystal-based time delay unit for phased array antennas," *Journal of Lightwave Technology*, Vol. 15, No. 7, July 1997.
13. N. A. Riza, "25 Channel nematic liquid crystal optical time-delay unit characterization," *IEEE Photonics Technology Letters*, Vol. 7, No. 11, pp. 1285-1287, November 1995.
14. N. Madamopoulos and N. A. Riza, "Switched three dimensional photonic delay line using directly modulated semiconductor lasers for microwave radar processing," *SPIE Proc.*, Vol. 2845, pp. 266-275, 1996.
15. C. H. Cox, "Gain and noise figure in analogue fibre-optic links,"*IEE Proceedings-J*, Vol. 139, No. 4, August 1992.
16. N. Madamopoulos, and N. A. Riza, "Adaptable Delay Balanced Switched Photonic Control Modules for Antenna Arrays," *SPIE Proc.*, Vol. 3160, No. 8, 1997.
17. N. A. Riza and N. Madamopoulos, "Photonic time delay beamforming architectures using polarization switching arrays," *SPIE Proc.*, Vol. 2754, pp. 186-197, 1996.
18. J. Kim, N. A. Riza, "Fiber array optical coupling design issues for photonic beamformers," *SPIE Proc.*, Vol. 2754, pp. 271-282, 1996.